Tausendfreund, Andreas ; Stöbener, Dirk ; Fischer, Andreas

# Speckle photographic in-process measurement of three-dimensional deformations in running manufacturing processes

| | | |
|---|---|---|
| Conference paper | as: | published version (Version of Record) |
| DOI of this document*(secondary publication): | | https://doi.org/10.26092/elib/3652 |
| Publication date of this document: | | 07/02/2025 |

* for better findability or for reliable citation

Recommended Citation (primary publication/Version of Record) incl. DOI:

Andreas Tausendfreund, Dirk Stöbener, and Andreas Fischer "Speckle photographic in-process measurement of three-dimensional deformations in running manufacturing processes", Proc. SPIE 11782, Optical Measurement Systems for Industrial Inspection XII, 1178205 (20 June 2021); https://doi.org/10.1117/12.2592284

# Speckle photographic in-process measurement of three-dimensional deformations in running manufacturing processes

Andreas Tausendfreund[*a], Dirk Stöbener[a,b], Andreas Fischer[a,b]
[a]University of Bremen, Bremen Institute for Metrology, Automation and Quality Science, Linzer Str. 13, 28359 Bremen, Germany
[b]University of Bremen, MAPEX Center for Materials and Processes, P.O. 330440, 28334 Bremen, Germany

## ABSTRACT

The concept of process signature uses the relationship between a material load and the resulting modification remaining in the workpiece to better understand and optimize manufacturing processes. The metrological recording of the loads occurring during the machining process in the form of mechanical deformations is the basic prerequisite for this approach. An appropriate characterization method is speckle photography, which is already applied for in-plane deformation measurements in various manufacturing processes. A shortcoming of this fast and robust measurement technique based on image correlation techniques is that deformations in the direction of the measurement system are not detected and that they increase the error of measurement for in-plane deformations. Therefore, this work investigates a method that infers local out-of-plane motions of the workpiece surface from the decorrelation of speckle patterns and thus is able to reconstruct three-dimensional deformation fields. The implementation of the evaluation method in existing sub-pixel interpolation algorithms enables a fast reconstruction of 3D deformation fields, so that the desirable in-process capability remains given. Using a deep rolling process, first measurements show that dynamic 3D-deformations below the tool can be detected, which confirms the suitability of the speckle photography not only for the 2D- but also the 3D-analysis of deformations in manufacturing processes.

**Keywords:** speckle photography, in-process measurement, rolling process

## 1. INTRODUCTION

The functionality of technical surfaces is significantly influenced by the manufacturing process [1,2,3]. In particular, this applies to processes, which aim to change the surface layer properties of the workpiece in a suitable manner. Currently, the targeted generation of e.g. hardness depth gradients is still a challenge - even under laboratory conditions [2]. The reasons for observed property deviations are that the material loads occurring during the machining process in the form of displacements and strains, which are responsible for the material changes, cannot be measured and that there is a lack of process knowledge. Therefore, the targeted material changes have been achieved so far only by iteratively adjusting the machining parameters or process variables of the machine tools [4,5,6]. This is remedied by the introduced concept of process signatures [7], which targets the internal mechanisms and the influencing variables [8] to describe the workpiece modification. The basis for the process signature concept is the correlation of the occurring material changes with the acting internal mechanical material loads. The use of process signatures not only allows a better understanding of the process, but also a comparison of seemingly different manufacturing processes. This enables different processes and process chains to be combined and optimized to improve functional properties and reduce costs in manufacturing [7].

While there is a multitude of characterization methods for the resulting material modifications, the metrological recording of the material loads during the ongoing production process remains a challenge. By comparing or correlating images taken before and during the occurrence of deformation, mechanical workpiece loads can be calculated with the methods of Digital Image Correlation (DIC) or Digital Speckle Photography (DSP). In contrast to DIC, the DSP method [9] is much more accurate, especially for low-contrast surfaces. Regarding the maximum achievable resolution, the method is only limited by the Heisenberg uncertainty principle [10]. Indeed, the in-process capability and suitability of the speckle photography method for two-dimensional deformation measurement in the image plane with resolutions of less than 20 nm [11] has

[*] a.tausendfreund@bimaq.de

Optical Measurement Systems for Industrial Inspection XII, edited by Peter Lehmann, Wolfgang Osten, Armando Albertazzi Gonçalves, Proc. of SPIE Vol. 11782, 1178205
 · doi: 10.1117/12.2592284

already been demonstrated in several manufacturing applications [12,13,14,15]. But since mechanical processing induces at least a biaxial stress state and hence a triaxial strain state in the workpiece via the machining forces, a reconstruction of three-dimensional deformation fields is required for a complete metrological description of the loads.

Although the original speckle photography is only suitable for two-dimensional in-plane measurements, there are several derivates of the method available to obtain out-of-plane deformation information, too. In this context, Khodadad et al. propose a combination of speckle photography and speckle interferometry [16]. Their robust setup uses only one camera and can determine three-dimensional displacements with a resolution of 0.6 µm but employs two evaluation algorithms increasing the evaluation complexity. Another method presented by Fricke-Begemann [17] uses the decorrelation of speckle patterns associated with out-of-plane motion, i.e., the speckle correlation functions changing with motion are evaluated. The measurement uncertainties determined here are in the range of one tenth of the wavelength and thus are significantly lower than those obtained with the approach of Khodadad.

The objective of this work is to realize a solely speckle-photographic in-process measurement system for the acquisition of three-dimensional load fields without a significant increase of the evaluation complexity and time. As a first practical implementation, the deformation fields in the manufacturing process of deep rolling are to be measured. Pending questions related to speckle-photographic 3D deformation measurement in manufacturing processes are to what extent such a measurement system is suitable for use in the harsh manufacturing environment and in which way the proposed algorithms are sufficient for in-process measurement. The functional relationship between speckle decorrelation and displacements in the out-of-plane axis and the calibration of this axis must also be investigated.

This paper is accordingly structured as follows: Section 2 describes the challenges of three-dimensional deformation measurement using speckle photography, especially in the Fricke-Begemann deformation evaluation. In addition, an alternative approach and its implementation in the context of sub-pixel interpolation is presented. After the demonstration of calibration strategies, first in-process measurements during deep rolling with the corresponding reconstruction of the three-dimensional deformation or displacement field follow in section 3. Finally, a summary and outlook is given in Section 4.

## 2. THEORY AND METHODS

### 2.1 In-plane speckle photography

If a rough surface is illuminated with a plane monochromatic wave, a so-called speckle pattern is created in the image plane of an imaging camera system by constructive and destructive interference (see zoomed area $W_{eval}$ in Figure 1). In this case, each surface point on the object surface is assigned the coordinates $\xi$ and $\psi$, to a point $(x,y)$ on the camera chip. When an occurring material deformation shifts a point $(\xi,\psi)$ on the measured surface by $\Delta\xi$ or $\Delta\psi$, the corresponding point $(x,y)$ in the image plane shifts by $\Delta x$ or $\Delta y$, respectively. This displacement can be determined via the maximum position of the cross-correlation function shown in Figure 1. To measure a global deformation field of many object points in a region of interest $W_{FOV}$, a small local evaluation window $W_{eval}$ is rasterized over the entire image $W_{FOV}$ and the displacement is determined in it.

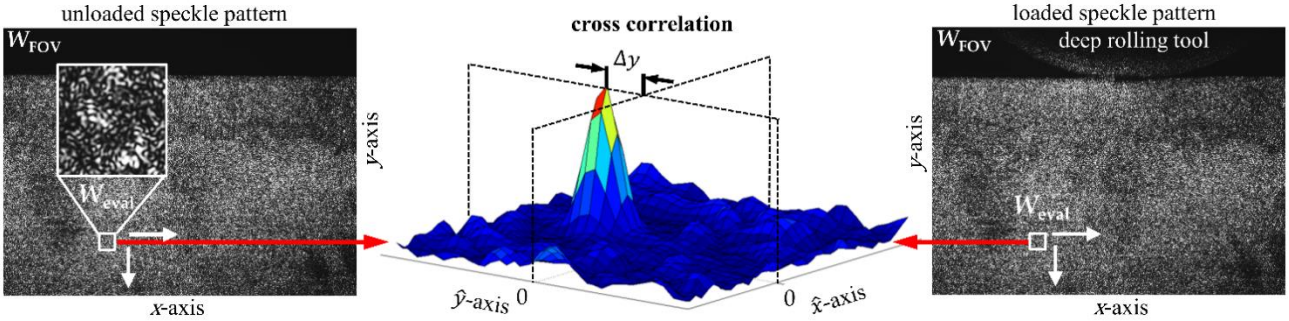


Figure 1. Evaluation principle of speckle photography for two-dimensional in-plane deformation measurement. Speckle pattern when viewing the unloaded workpiece (left) and speckle pattern of a stressed workpiece under load (right).

For determining the position of the maximum of the cross-correlation shown in Figure 1 with sub-pixel accuracy, interpolation methods based on curve approximation are used. The actually applied sub-pixel interpolation algorithm by Nobach and Honkanen [18] determines the displacement of the maximum $(\Delta x, \Delta y)$ using an elliptic Gaussian function

$$g(\hat{x},\hat{y}) = a \cdot \exp\{b_{20}(\hat{x}-\Delta x)^2 + b_{11}(\hat{x}-\Delta x)(\hat{y}-\Delta y) + b_{02}(\hat{y}-\Delta y)^2\}, \quad (1)$$

with variables $(\hat{x},\hat{y})$ fitted to the cross-correlation function. It can be rewritten as:

$$g(\hat{x},\hat{y}) = \exp\{c_{00} + c_{10}\hat{x} + c_{20}\hat{x}^2 + c_{01}\hat{y} + c_{11}\hat{x}\hat{y} + c_{02}\hat{y}^2\} \quad (2)$$

with

$$c_{00} = \ln(a) + b_{20}\Delta x^2 + b_{11}\Delta x\Delta y + b_{02}\Delta y^2, \quad (3)$$

$$c_{10} = -2b_{20}\Delta x - b_{11}\Delta y, \quad (4)$$

$$c_{20} = b_{20}, \quad (5)$$

$$c_{01} = -b_{11}\Delta x - 2b_{02}\Delta y, \quad (6)$$

$$c_{11} = b_{11}, \quad (7)$$

$$c_{02} = b_{02}. \quad (8)$$

The shift components $\Delta x$, $\Delta y$ of the maximum are then obtained from the equations (3-8) as follows [18]:

$$\Delta x = \frac{c_{11}c_{01} - 2c_{10}c_{02}}{4c_{20}c_{02} - c_{11}^2} \quad (9)$$

$$\Delta y = \frac{c_{11}c_{10} - 2c_{01}c_{20}}{4c_{20}c_{02} - c_{11}^2} \quad (10)$$

The relationship between the displacement $\Delta x$, $\Delta y$ in the image plane and the respective object displacement $\Delta\xi$, $\Delta\psi$ within the measuring area is linear. With the magnification factor $A$ of the lens system used, it can be written as:

$$\Delta\xi = A\,\Delta x \quad (11)$$

$$\Delta\psi = A\,\Delta y \quad (12)$$

### 2.2 Three-dimensional speckle photography in out-of-plane direction

Obtaining information about the 3D deformation field is essential for the initially targeted objective of an extended understanding of the manufacturing process. Speckle photographic approaches are in principle also well suited for this purpose, since the recorded speckle patterns basically represent sections through the three-dimensional structure of the wave field. The exemplary measured three-dimensional structure of the speckle pattern, for a $\zeta$-shift of the measurement plane consisting of camera plane and illumination plane is shown in figure 2a.

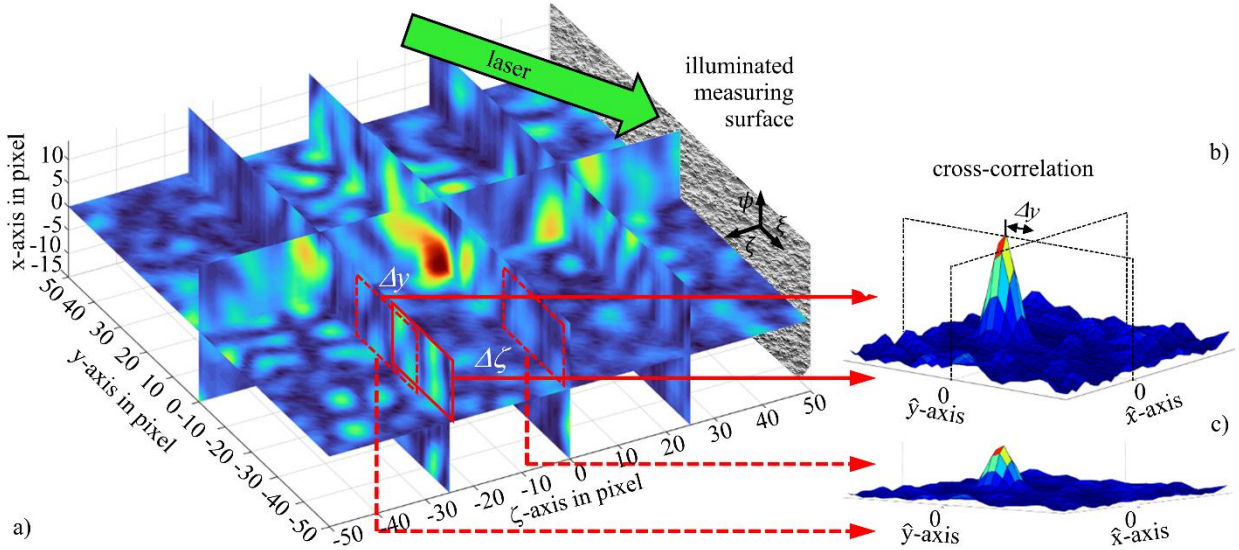


Figure 2. 3D speckle pattern measured by the shift of the illumination and the camera system in the $\zeta$-axis (a) and the calculated cross-correlation function of two evaluation windows shifted against each other in the $y$-direction (b) or in the $\zeta$-direction (c).

For pure in-plane displacements $\Delta\xi$, $\Delta\psi$, the cross-correlation is shown in Figure 2b. In contrast, displacements and deformations of the surface in the out-of-plane direction ($\Delta\zeta$) lead to a decorrelation of the speckle patterns, i.e. to a reduced amplitude of the cross-correlation maximum (see Figure 2b and 2c). This decorrelation was previously regarded as a disturbance of the measurement effect and minimized by higher measurement rates. The Fricke-Begemann approach exploits the decorrelation and derives the out-of-plane deformation of the measurement surface via an elaborate shape analysis of the power spectrum of the cross-correlated speckle patterns [17]. Maximum likelihood estimation is first used to determine the tilt angles of the surface points and, based on this, comprehensive three-dimensional deformation measurements are finally reconstructed. But laboratory studies of simultaneous tilts and in-plane displacements of the measurement surface illustrate the problem that arises in this form of evaluation when tilts and in-plane displacements are separated, see Figure 3.

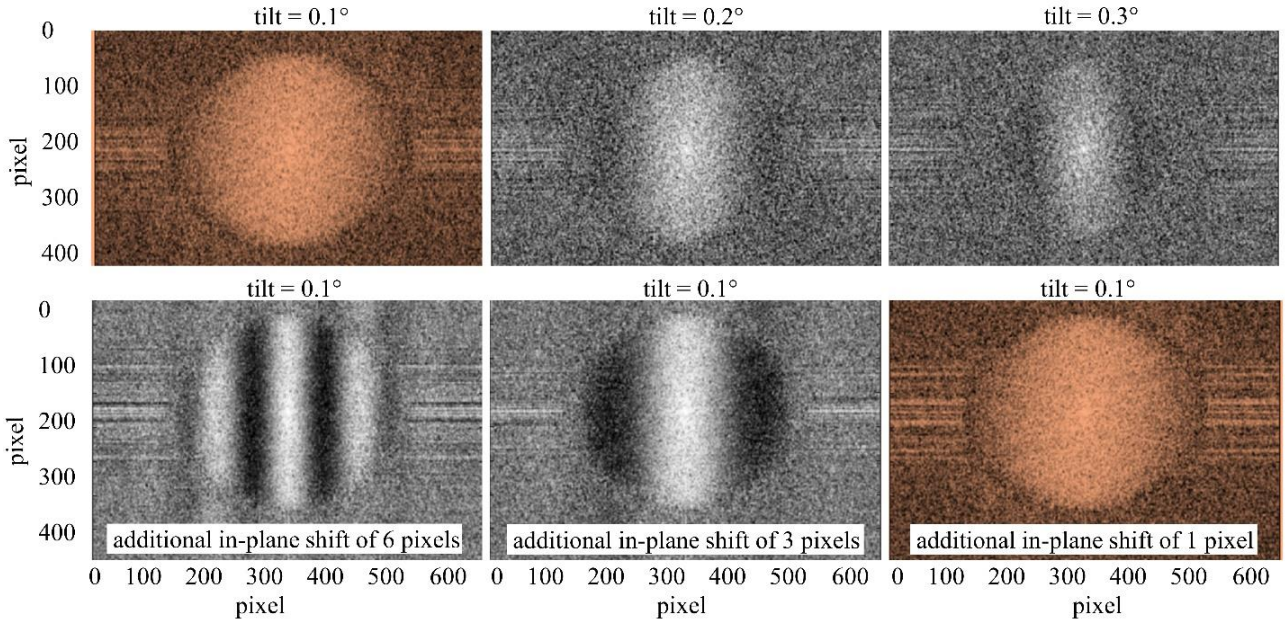


Figure 3. Laboratory investigation of tilting and simultaneous displacement of the measurement surface. Shown are the power spectra of two speckle patterns for surfaces that are tilted or displaced relative to each other.

Particularly in the range of very small displacements (< 1 pixel), which are predominant in in-process load measurements of manufacturing processes, the differences are hardly noticeable (see red colored areas in Figure 3). While in-plane shifts in the cross-correlation (see Figure 1) can be clearly seen in the shift of the maximum – without significantly affecting the shape of the curve –, in the evaluation via the power spectrum both the in-plane shift and the out-of-plane movement affect the shape of the curve. Although the power spectrum is very sensitive to the tilts, complex fit and filter algorithms are required to separate the two components. First approaches for the analysis of a two-axis motion, which consists of a tilt in the $\xi$-axis and a displacement in $\psi$-direction, resulted in computation times in the double-digit minute range for the smallest evaluation windows. In view of the parallelization of the evaluation algorithms and the goal of a fast in-process measurement, an alternative approach is therefore pursued. Cross-correlation enables the separation of in-plane and out-of-plane shift information by evaluating the shift of the correlation maximum (see Figure 2b) or the broadening of the normalized cross-correlation function (see Figure 2c). The shape or the width of the correlation function is already evaluated in connection with the performed subpixel interpolation. In the time-optimized interpolation, the width $\sigma$ of the approximated Gaussian function $g(\hat{x}, \hat{y})$ is inherently hidden. It can be considered as the value for the speckle decorrelation and thus for the out-of-plane deformation. According to equations (1,5,8), the width components for the $\hat{x}$ and $\hat{y}$ directions, respectively, are as follows

$$\sigma_{\hat{x}} = \sqrt{\frac{1}{-2c_{20}}}, \tag{13}$$

$$\sigma_{\hat{y}} = \sqrt{\frac{1}{-2c_{02}}}. \tag{14}$$

While the functional relationship between the displacement of the maximum of the cross-correlation function and the in-plane displacement of a surface point is linearly related via the magnification factor $A$, the functional relationship between the out-of-plane shift $\Delta\zeta$ and the width of the correlation function $\sigma_x$ or $\sigma_y$ is unknown yet. To determine a corresponding calibration function, the relationship $\Delta\zeta(\sigma_x,\sigma_y)$ is investigated experimentally in the following.

### 2.3 Relationship between the width of the correlation function and the out-of-plane shift

To analyze the functional relationship $\Delta\zeta(\sigma_x,\sigma_y)$, a laboratory setup of a speckle-photographic measurement system was realized, see Figure 4a. A collimated illumination of the measured object, a sandblasted sheet metal strip (400 mm x 50 mm), is performed with a widened *Omicron* laser ($\lambda$ = 405 nm). The illuminated measuring field is observed and imaged with an *Imaging Source* camera (DMK 21AU04) through a *Pentax* 25 mm lens. Camera, laser and the center of the sheet metal strip (in the center of the measurement field) are fixed on a linear axis from *PI* company. On the other hand, the outer ends of the sheet metal strip are fixed to the laboratory bench. Therefore, a movement of the linear axis causes a bending of the sheet metal strip (yellow line in Figure 4a) and thus a relative movement between the center and its outer ends.

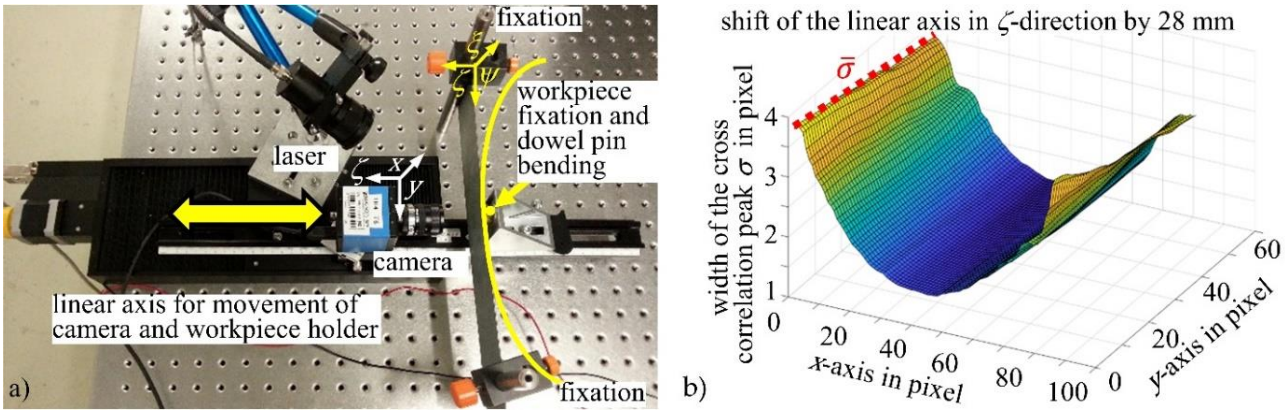


Figure 4. Investigations on the width of the correlation function for decorrelated speckle patterns: (a) laboratory setup with indicated bending of the workpiece sheet over a locating pin fixed in the camera system (yellow) and (b) the resulting global field of the respective local widths of the correlation functions when the linear axis is displaced by 28 mm.

Figure 4b illustrates the global field of the respective locally calculated correlation function widths

$$\sigma = \sqrt{\sigma_x^2 + \sigma_y^2} = \sqrt{\frac{1}{-2c_{20}} + \frac{1}{-2c_{02}}} \tag{15}$$

for a linear axis displacement of 28 mm in $\zeta$-direction with a total measurement field size of 30 mm x 40 mm. The parabolic bending around the dowel pin in the center of the image is very well recognizable. From the original 1.3 pixels, the width of the correlation function increases significantly to approximately 4 pixels. When looking at the pixels along the $y$-axis at the position $x = 0$ in Figure 4b, one can see the linear relationship shown in Figure 5 between the respective displacement of the linear axis and the mean broadening of the interpolated correlation function $\bar{\sigma}$.

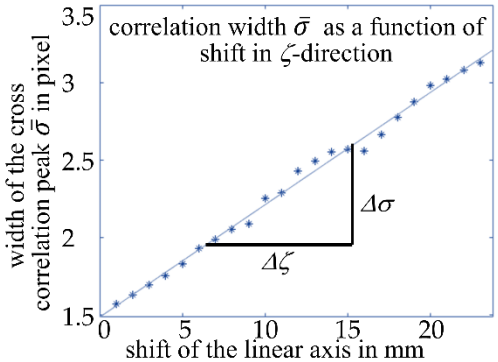


Figure 5. Linear relationship between the width of the correlation function $\bar{\sigma}$ calculated in the sub-pixel interpolation and the shift of the linear axis in $\zeta$-direction.

Thus, the functional relationship between a changed loading condition with a resulting displacement $\Delta\zeta$ and the resulting speckle decorrelation or change in the width $\Delta\sigma$ of the Gaussian fit $g(\hat{x}, \hat{y})$ from equation (1) is linear in nature and results in:

$$\Delta\zeta = \pm B\,\Delta\sigma \tag{16}$$

The reason for the undetermined sign of the calibration factor $B$ results intuitively from Figure 2. The displacement by $+\Delta\zeta$ leads to the decorrelation of the speckle pattern to the same extent as a displacement by $-\Delta\zeta$. While the calibration factor can be defined before a respective measurement on the basis of a defined displacement, the sign can be determined only by prior knowledge of the observed deformation process. For example, in the case of the bending test, the outer ends of the sheet metal strip will move away from the camera in the negative $\zeta$-direction, so negative signs would be expected. Just as the in-plane deformation $(\Delta\xi,\Delta\psi)$ is linearly related to the shift of the maximum $(\Delta x,\Delta y)$ of the cross-correlation via the magnification factor $A$ (equations (11) and (12)), it could be shown by equation (16) that such a simple linear relationship also results for the out-of-plane deformation $\Delta\zeta$ via the factor $B$ and the width change of the cross-correlation function $\Delta\sigma$.

## 3. IN-PROCESS MEASUREMENT IN A DEEP ROLLING PROCESS

### 3.1 Measurement setup and experimental realization

As the first manufacturing process, the deep rolling process was selected due to the expected strong out-of-plane movement in the edge area of the machined surface. The production process was replicated in a laboratory set-up, which is shown together with the measurement set-up in Figure 6.

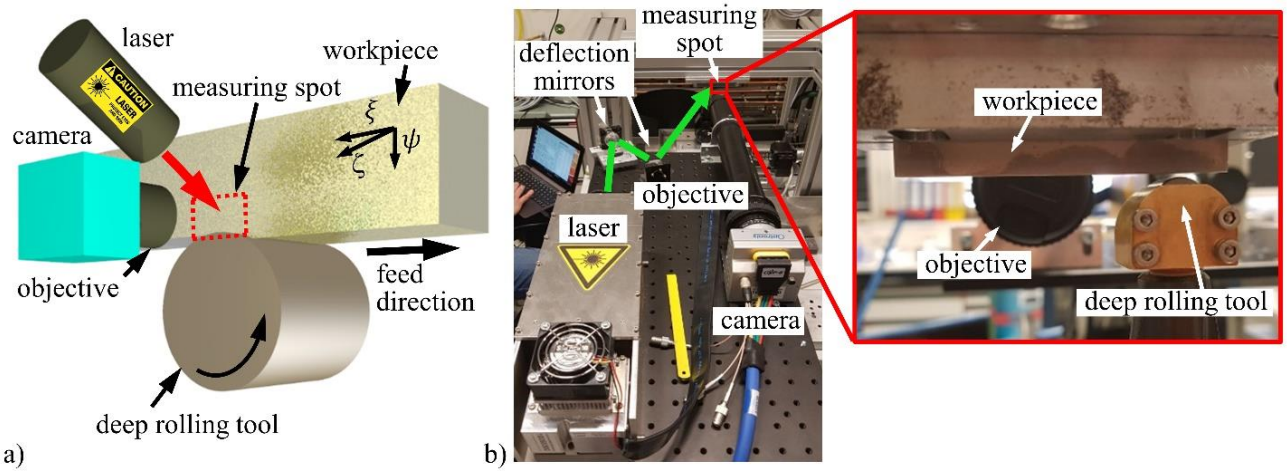


Figure 6. Experimental setup for deep rolling: Principle measurement setup (a) and practical implementation with magnified view from the opposite direction to the camera (b).

The setup is also used for in situ X-ray diffraction analysis and residual stress measurement and is described in detail in [19]. In contrast to the intuitive idea, the setup is upside down and the rolling tool presses on the workpiece from below, so that any cooling lubricant escaping from the hydraulic rolling tool is prevented by gravity from contaminating the measuring field located on the front surface of the workpiece and disturbing the measurement. The axis of rotation of the cylindrical tungsten carbide tool with a diameter of 13 mm, which protrudes a few millimeters above the workpiece, is parallel to the $\zeta$-axis of the specimen or measuring system. The $\xi\psi$-plane lies in the face of the hardened martensitic 42CrMo4 workpiece (150 mm x 70 mm x 20 mm). While rolling, the tool moves with a loading of 350 bar in the negative $\xi$-direction at a feed rate of v = 0.02 mm/s (Figure 6a). The measuring field of 8 mm x 6 mm is illuminated by a short pulse laser ($t_p$ = 1 ns, $\lambda$ = 532 nm) from *Horus* via two deflection mirrors and observed with a 4K high speed camera CP70 from *Optronis* through a 90 mm Apo-Rodagon lens from *Rodenstock* (see Figure 6b). In the rolling process with its moderate feed rate, full-frame recordings with a recording rate of 166 frames per second could be made.

### 3.2 Results of 3D-deformation measurements

Results of a three-dimensional load measurement for the deep rolling experiment are shown in Figure 7. Under the assumption of a homogeneous workpiece, the evaluation range in $\xi$-direction is extended from 8 mm to 20 mm. In order to do this, the speckle-photographic deformation measurements of the time series - in the direction of movement of the tool - were combined to form an extended evaluation field [15, 20]. According to equations (11) and (12), the calibration of the $\xi$- and $\psi$-axis is performed from the magnification $A$ of the lens system.

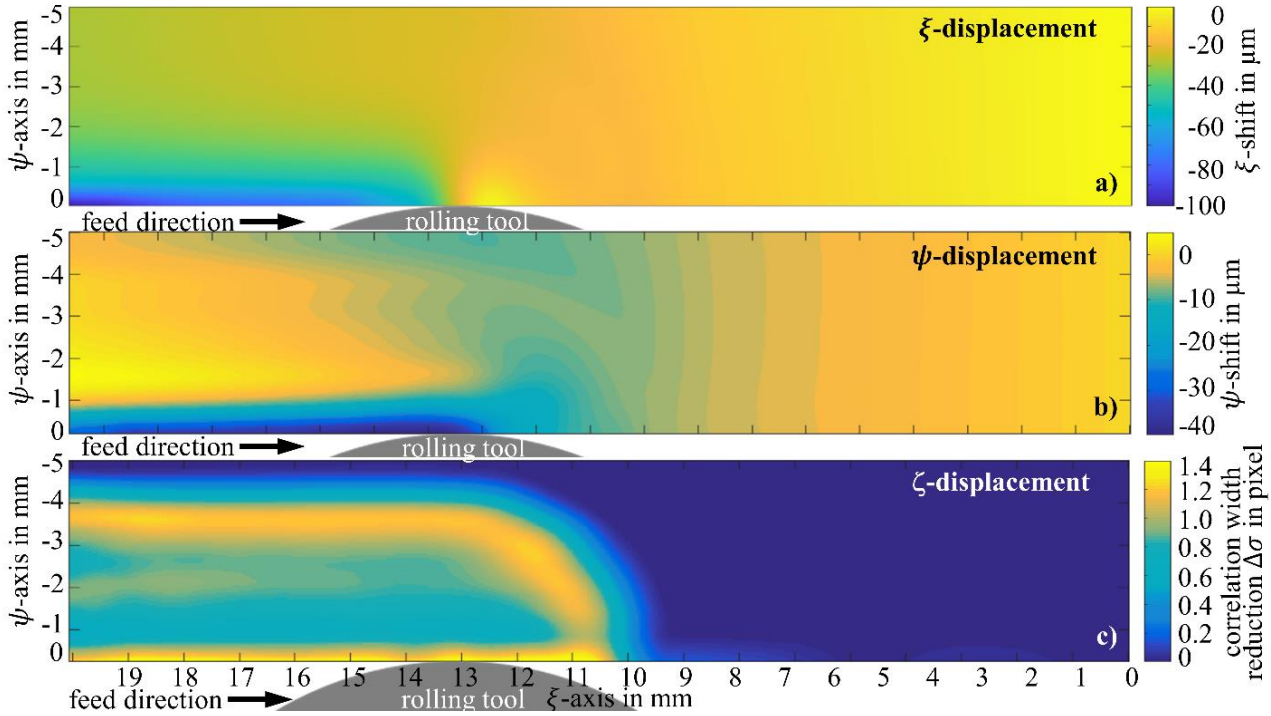


Figure 7. In-process measurement in the deep rolling process: Shown are the occurring shifts in $\xi$-direction (a) and $\psi$-direction (b) as well as the reduction of the width of the correlation function $\Delta\sigma$ calculated in the sub-pixel interpolation as a value for the $\zeta$-shift (c) resulting from the out-of-plane deformation.

During the deep rolling process, the load measurements show maximum deformation differences for the $\xi$- and $\psi$-direction at a depth of 800 µm. Consequently, the equivalent stress maximum also occurs at this depth, which corresponds to the expectations [19]. The material on the machined surface moves up to 100 µm in the direction of tool movement (Figure 7a). In $\psi$-direction the maximum displacement is located about 1 mm behind the contact point of the tool at position 14 mm and is 40 µm (Figure 7b). For the first time, in addition to the measured in-plane deformations in $\xi$- and $\psi$-direction, now Figure 7c also shows the out-of-plane component of the in-process characterization in the direction of the camera axis. This shift in $\zeta$-direction corresponds to the broadening of the correlation function $\Delta\sigma$ or a decorrelation of the speckle patterns between unloaded and loaded state.

In particular, the significant decorrelation at a depth of 3-4 mm previously hindered the correct interpretation of the measurement data. The measurement rate was therefore increased until no significant decorrelation occurred. With regard to the $\Delta\xi$- and $\Delta\psi$- evaluation, the increase of the measuring rate was mostly at the expense of the lateral measuring point density or also at the expense of the displacement resolution in the respective evaluated direction. Note the difference between the lateral measurement point density, which is given only by the size of the evaluation windows, and the displacement resolution, which depends on various quantities such as speckle size or camera noise [13].

To obtain a complete description of the three-dimensional displacement field, the only remaining task is to perform the calibration between the $\Delta\zeta$-displacement and the decrease of the correlation width $\Delta\sigma$ according to equation (16). The scaling or calibration of the $\zeta$-axis is performed in this case by a subsequent reference measurement with a stylus instrument (*Mahr* LD-120). In order to do this, the tactilely measured burr (see Figure 8a) was compared with the determined width of the correlation function (see Figure 8b). The approximately linear deformation of the burr shown in the section is

reflected proportionally in the linear behavior of the correlation width $\Delta\sigma$ and confirms the preliminary tests from Figure 5. For this reason, a linear correlation is also assumed for the speckle photographic measurement in Figure 8c and the $\zeta$-axis is scaled accordingly. The evaluation of the speckle decorrelation in principle does not give any information about the sign of the measured $\Delta\zeta$-deformation (see section 2.3). The evaluation succeeds, however, due to the prior knowledge gained from the calibration measurements that the material is pressed outward in the direction of the camera.

Figure 8c clearly shows the strong burr formation at the edge of the workpiece with an extension of up to 80 µm, caused by the high rolling pressure of 350 bar applied to the 42CrMo4 specimen. The dynamic deformation front, which propagates like a 'bow wave' in front of the die, is highlighted in the measured data. This dynamic deformation front is exactly what has caused problems in the interpretation of the measured data so far, as the associated decorrelation of the speckle patterns could not be explained. Overall, the acquisition of the load dynamics shows that speckle photography is suitable for measuring and evaluating three-dimensional deformation fields within ongoing manufacturing processes. Especially the analysis of the loading dynamics is a key to identify the process signatures described above as well as to compare them with corresponding simulations of the manufacturing process and illustrates the great potential of this in-process measurement technique.

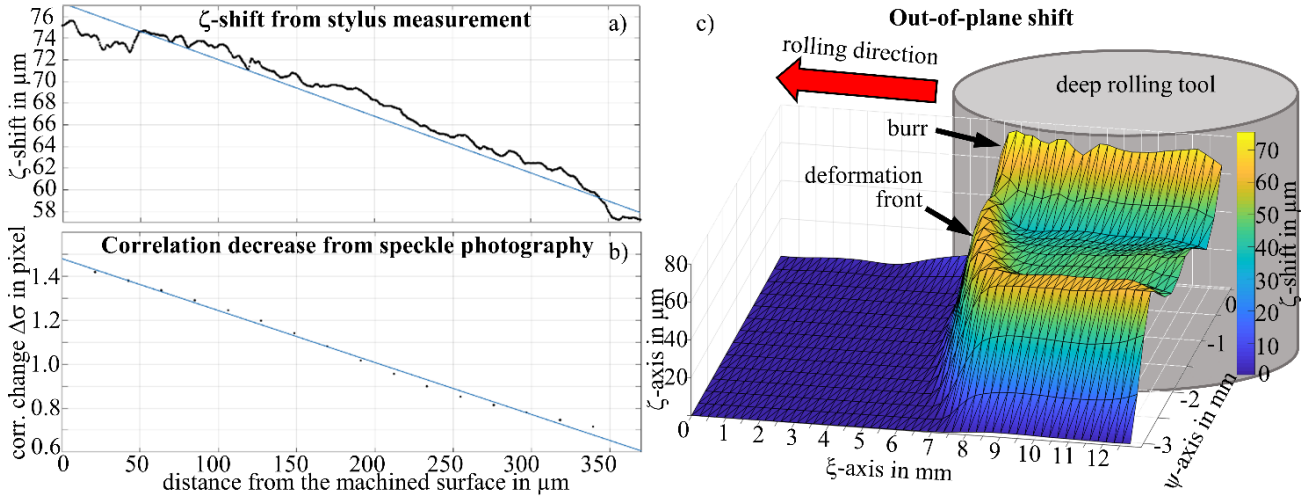


Figure 8. Three-dimensional deformation measurement in the deep rolling process. a) tactile measured burr; b) width of the correlation function depending on the out-of-plane displacement of the burr; c) speckle-photographically measured deformation field in $\zeta$-direction after calibration.

## 4. CONCLUSION AND OUTLOOK

In the context of the analysis of the functional relationship between the decorrelation of measured speckle patterns or the broadening of the correlation function and the out-of-plane deformation, laboratory investigations confirm a linear behavior. Furthermore, the additional computational effort for the determination of the subpixel analysis is negligible, so that the parallelizability of the algorithms remains given and three-dimensional in-process deformation measurements during the rolling process become possible. The measurements during deep rolling show the dynamic deformations below the die. Based on these deformations, the strain and thus the load during the tool engagement can be calculated directly via gradient formation. Particularly the 'bow wave' of out-of-plane deformation moving in front of the tool shows that the local mechanical material stresses can be much more pronounced than the workpiece changes remaining in the material. For better understanding of manufacturing processes, 3D speckle photography can thus make an important contribution in the context of process signatures.

Calibration of the $\xi$- and $\psi$-displacement can be performed via the imaging scale of the camera system, but for the $\zeta$-axis this is only possible via a subsequent reference measurement with a stylus instrument. Also, the ambiguity regarding the direction of the displacement can be eliminated by the additional information from the reference measurement. For the future, the realization of a self-calibration of the measuring system is planned in order to ensure the in-process capability in different manufacturing processes. This will be achieved by using a three-axis piezo stack, via which the system can be

calibrated before each individual measurement by means of defined, homogeneous deflections. Beside the calibration, it is thus simultaneously possible to eliminate optical distortions – for example due to misalignments of the measuring system – already while measuring and to perform quantitative 3D deformation measurements during the running machining process.

**Author Contributions:**

A. Tausendfreund performed the experiments, designed the measurement setup and analyzed the data. All authors elaborated the measurement technology with its implementation and participated in the elaboration and discussion of the manuscript.

**Acknowledgements**

The authors gratefully acknowledge the financial support by the German Research Foundation (DFG) for subproject C06 'Surface optical measurement of mechanical working material loads' within the Transregional Cooperative Research Center SFB/TRR136. They also thank Heiner Meyer (subproject C01) and their colleagues from the Leibniz Institute for Materials Engineering IWT for the friendly support during the conduction of the in-process measurements.

## REFERENCES

[1] Field, M. and Kahles, J.F., "Review of Surface Integrity of Machined Components," CIRP Ann.-Manuf. Techn., 20(2), 153-163 (1971).
[2] Jawahir, I.S., Brinksmeier, E., M'Saoubi, R., Aspinwall, D.K., Outeiro, J.C., Meyer, D., Umbrello, D. and Jayal, A.D., "Surface integrity in material removal processes: Recent advances," CIRP Ann.-Manuf. Techn., 60(2), 603-626 (2011).
[3] Habschied, M., de Graaff, B., Klumpp A. and Schulze, V., „Fertigung und Eigenspannungen," HTM J Heat Treatm. Mat., 70(3), 11-121 (2015).
[4] Liang, S.Y. and Su, J-C., "Residual Stress Modeling in Orthogonal Machining," CIRP Ann.-Manuf. Techn., 56(1), 65–68 (2007).
[5] Lazoglu, I., Ulutan, D. and Alaca, B.E., "An enhanced analytical model for residual stress prediction in machining," CIRP Ann.-Manuf. Techn., 57(1), 81-84 (2008).
[6] Brinksmeier, E., Heinzel, C., Garbrecht, M., Sölter, J. and Reucher, G., "Residual Stresses in High Speed Turning of Thin-Walled Cylindrical Workpieces," Int. J. Autom. Technol., 5(3), 313-319 (2011).
[7] Brinksmeier, E., Klocke, F., Lucca, D.A., Sölter, J. and Meyer, D., "Process Signatures - a New Approach to Solve the Inverse Surface Integrity Problem in Machining Processes," Procedia CIRP, 13, 429-434 (2014).
[8] Greenwood, G.W. and Johnson, R.H., "The deformation of metals under small stresses during phase transformations," Proc. Roy. Soc., 283A, 403-422 (1965).
[9] Parks, V. J., "The range of speckle metrology," Experimental Mechanics, 20(6), 181-191 (1980).
[10] Fischer, A., "Fundamental uncertainty limit of optical flow velocimetry according to Heisenberg's uncertainty principle," Applied Optics, 55(31), 8787-8795 (2016).
[11] Tausendfreund, A., Stöbener, D. and Ströbel, G., "In-process measurements of strain fields during grinding," Proceedings of the 16th international conference of the european society for precision engineering and nanotechnology (euspen), Nottingham, 85-86 (2016).
[12] Tausendfreund, A., Borchers, F., Kohls, E., Kuschel, S., Stöbener, D., Heinzel, C. and Fischer, A., "Precise In-Process Strain Measurements for the Investigation of Surface Modification Mechanisms," Journal of Manufacturing and Materials Processing, (2018).
[13] Tausendfreund, A., Stöbener, D. and Fischer, A., "Precise In-Process Strain Measurements for the Investigation of Surface Modification Mechanisms," Journal of Manufacturing and Materials Processing, 2(1), (2018).
[14] Tausendfreund, A., Stöbener, D. and Fischer, A., "Induction of Highly Dynamic Shock Waves in Machining Processes with Multiple Loads and Short Tool Impacts," Applied Sciences, 9(11), 2293, (2019).
[15] Tausendfreund, A., Stöbener, D. and Fischer, A., "In-process workpiece deformation measurements under the rough environments of manufacturing technology," Procedia CIRP, (2020).

[16] Khodadad, D., Singh, A.K., Pedrini, G. and Sjödahl, M., "Full-field 3D deformation measurement: comparison between speckle phase and displacement evaluation," Applied Optics, 55(27), 7735-7743 (2016).
[17] Fricke-Begemann, T., "Optical measurement of deformation fields and surface processes with digital speckle correlation," Dissertation, University of Oldenburg, (2002).
[18] Nobach, H and Honkanen, M., "Two-dimensional Gaussian regression for sub-pixel displacement estimation in particle image velocimetry or particle position estimation in particle tracking velocimetry," Experiments in Fluids, 38, 511-515 (2005).
[19] Meyer, H. and Epp, J., "In Situ X-ray Diffraction Analysis of Stresses during Deep Rolling of Steel," Quantum Beam Science, 2(20), (2018).
[20] Tausendfreund, A., Stöbener, D. and Fischer, A., „Messung thermomechanischer Beanspruchungen in laufenden Schleifprozessen," tm-Technisches Messen, 87(3), 201-209 (2020).